

# Final state interaction effects in neutrino-nucleus quasielastic scattering

C. Maieron<sup>a</sup>, M.C. Martínez<sup>b</sup>, J.A. Caballero<sup>b</sup>, and J.M. Udías<sup>c</sup>

<sup>a</sup>Istituto Nazionale di Fisica Nucleare, Sezione di Catania, Via S. Sofia 64, I-95123 Catania, Italy

<sup>b</sup>Departamento de Física Atomica, Molecular y Nuclear, Universidad de Sevilla, E-41080 Sevilla, Spain

<sup>c</sup>Departamento de Física Atomica, Molecular y Nuclear, Universidad Complutense de Madrid, E-28040 Madrid, Spain

We consider the charged-current quasielastic scattering of muon neutrinos on an Oxygen 16 target, described within a relativistic shell model and, for comparison, the relativistic Fermi gas. Final state interactions are described in the distorted wave impulse approximation, using both a relativistic mean field potential and a relativistic optical potential, with and without imaginary part. We present results for inclusive cross sections at fixed neutrino energies in the range  $E_\nu = 200$  MeV - 1 GeV, showing that final state interaction effects can remain sizable even at large energies.

## 1. INTRODUCTION AND FORMALISM

A precise and realistic description of neutrino-nucleus interaction in the intermediate energy region is crucial for the interpretation of experimental results used to determine neutrino properties. At present most of the Monte Carlo codes [1] which have been developed to simulate the response of the detectors in these experiments are based on the Fermi gas model. Therefore they take into account the Fermi motion of the nucleons inside the nucleus and Pauli blocking effects, but they neglect several other effects, which are known to be important from electron scattering experiments [2].

In order to study the relevance of some of these effects, in this contribution we compare relativistic Fermi gas (RFG) calculations of neutrino-nucleus quasielastic scattering cross sections [3], with results obtained within a relativistic shell model (RSM), including, in particular, final state interactions (FSI) [4]. More details about our calculations can be found in Ref. [5]. FSI effects in  $\nu$ -nucleus scattering have also been studied in Refs. [6,7].

We consider the charged-current (CC) quasielastic scattering of muon neutrinos on  $^{16}\text{O}$  at fixed neutrino energies of 200, 500 and 1000 MeV, describing this process within the impulse approximation, schematically represented in fig. 1.

We thus assume that the incident neutrino interacts

with only one nucleon, which is then emitted, while the remaining (A-1) nucleons in the target are spectators, that the nuclear current is the sum of single nucleon currents and that the states of the target and residual nuclei are described by independent particle model wave functions. We describe the ground state of  $^{16}\text{O}$  as a closed shell configuration, the occupied shells being  $s_{1/2}$ ,  $p_{3/2}$  and  $p_{1/2}$ . For the removal of a nucleon from a closed shell of angular momentum  $j$ , the cross section corresponding to the diagram in fig. 1 has the following general form:

$$\frac{d^6\sigma}{d^3k'd^3p_N} = \int \delta^4(q + p_A - p_{A-1} - p_N) \frac{G_F^2}{(2\pi)^5} \quad (1)$$

$$\times \frac{(2j+1)}{8E_\nu E_\mu} \overline{\sum} |\bar{u}(k')\gamma^\alpha (1 + \gamma_5) u(k) J_\alpha(\mathbf{q})|^2 d^3p_{A-1},$$

where  $G_F$  is the Fermi constant,  $\overline{\sum}$  indicates the average/sum over the initial/final spins,  $\gamma_5 = -i\gamma^0\gamma^1\gamma^2\gamma^3$  and Dirac spinors are normalized according to  $u(k)^\dagger u(k) = 2k_0$ . We then sum over the occupied shells and integrate over the emitted nucleon and over the direction of the outgoing muon in order to get the inclusive cross sections  $d\sigma/dT_\mu$ , and the integrated inclusive cross section  $\sigma = \int (d\sigma/dT_\mu) dT_\mu$ ,  $T_\mu$  being the outgoing lepton kinetic energy.

The main ingredient in eq. (1) is the single nucleon

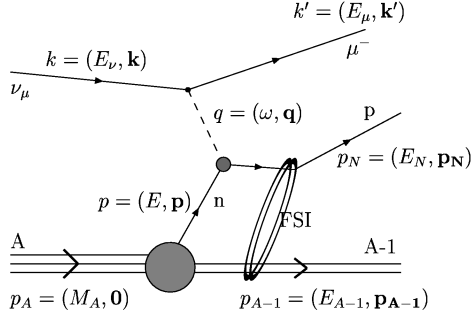


Figure 1. Born approximation diagram for CC  $\nu$ -nucleus quasielastic scattering. The impulse approximation is assumed in the hadronic vertex and the possibility of final state interactions between the outgoing nucleon and the residual nuclear system is explicitly shown.

current matrix element,

$$J_\alpha(\mathbf{q}) = \sqrt{V} \int d^3r e^{i\mathbf{q}\cdot\mathbf{r}} \bar{\psi}_{s_N}(\mathbf{p}_N, \mathbf{r}) \hat{\Gamma}_\alpha \psi_B^{jm}(\mathbf{r}), \quad (2)$$

where  $\psi_B^{jm}(\mathbf{r})$  and  $\psi_{s_N}(\mathbf{p}_N, \mathbf{r})$  are the wave functions for the initial (bound) nucleon and for the emitted nucleon, respectively, and  $\hat{\Gamma}_\alpha$  is the single nucleon weak charged-current operator. For the latter we assume the free, on mass shell, nucleon expression:

$$\hat{\Gamma}_\alpha = |V_{ud}| \left[ F_V \gamma_\alpha + F_M \frac{i}{2m_N} \sigma_{\alpha\beta} q^\beta \right. \\ \left. + F_A \gamma_\alpha \gamma_5 - F_P q_\alpha \gamma_5 \right], \quad (3)$$

where  $F_{V,M}$  are the CC single nucleon Pauli and Dirac form factors,  $F_A$  and  $F_P$  are the axial and the induced pseudoscalar form factor, respectively, and  $|V_{ud}|$  is the  $ud$  Cabibbo–Kobayashi–Maskawa matrix element. For  $F_A$  we assume a dipole parameterization with cutoff mass  $M_A = 1.026$  GeV.

In eq. (2) the bound nucleon wave functions  $\psi_B^{jm}(\mathbf{r})$  are the self-consistent (Hartree) solutions of a Dirac equation, derived, within a relativistic mean field approach, from a Lagrangian containing  $\sigma$ ,  $\omega$  and  $\rho$  mesons, which has been already successfully used in

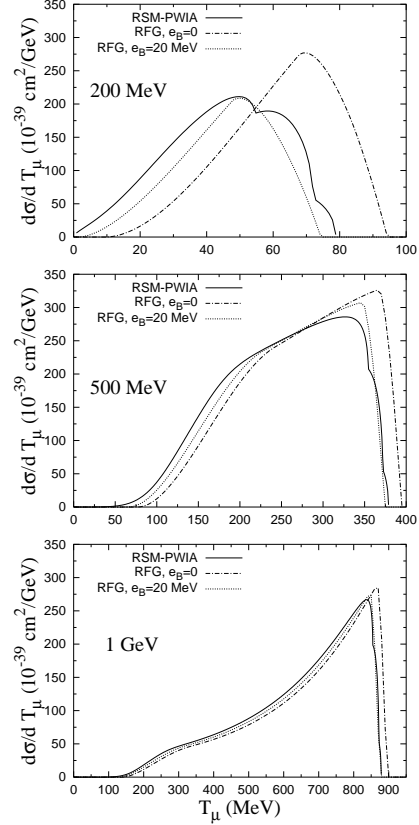


Figure 2. Differential cross section ( $d\sigma/dT_\mu$ ) versus the outgoing muon kinetic energy, for the quasielastic scattering of muon neutrinos on  $^{16}\text{O}$  and incident neutrino energy:  $E_\nu = 200$  MeV (upper panel), 500 MeV (middle) and 1 GeV (lower panel).

the study of  $(e, e'p)$  processes [4]. For the single-particle binding energies of the different shells we use the corresponding experimental values, which determine the threshold of the cross section for every shell.

Concerning the emitted nucleon, as a starting point we describe it as a plane wave, thus neglecting its interaction with the residual nucleus (plane wave impulse approximation - PWIA). Then, to make our description more realistic, we include the effects of FSI by using distorted waves (distorted wave impulse approximation - DWIA). For the latter, we make the following different choices.

*Complex ROP*: following previous studies of ex-

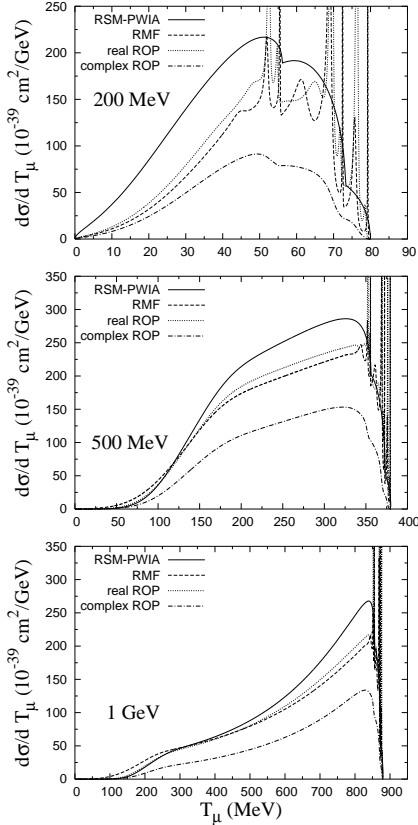


Figure 3. Same as fig. 2, but including FSI effects. All curves are calculated using the RSM model, in PWIA (solid) and describing FSI within the RMF (dashed), real ROP (dotted) and complex ROP (dot-dashed) approaches.

clusive electron scattering processes [4], we employ distorted waves which are obtained as solutions of a Dirac equation containing a phenomenological relativistic optical potential (ROP). The ROP has a real part, which describes the rescattering of the ejected nucleon and an imaginary part, that accounts for the absorption of it into unobserved channels.

*Real ROP:* since, contrary to the  $(e, e'p)$  case, here we are considering inclusive processes, where all final channels contribute, the presence of the imaginary term in the optical potential leads to an overestimation of FSI effects. For this reason we also consider the potential obtained by setting the imaginary part of the

ROP to zero (a discussion on the use of real optical potentials has been presented in Ref. [7]).

*RMF:* finally, we employ wave functions which are obtained as the solutions in the continuum of the same Dirac equation which is used to derive the bound nucleon wave functions. We refer to this approach as relativistic mean field (RMF) and consider it appropriate at low energy transfer.

## 2. RESULTS AND CONCLUSIONS

Let us now present the results we obtain for neutrino-nucleus quasielastic cross sections. As a first step we neglect FSI effects and just compare RSM-PWIA results with the corresponding curves obtained within the relativistic Fermi gas, for which we use a Fermi momentum  $p_F = 225$  MeV and binding energy  $e_B = 0$  or 20 MeV. This comparison is presented in fig. 2, where the differential cross sections  $d\sigma/dT_\mu$  is plotted as a function of the outgoing muon kinetic energy. We observe that the differences between the two models are quite large at low neutrino energy, but they practically disappear at  $E_\nu = 1$  GeV.

The situation is different if we “turn on” FSI effects, as illustrated in fig. 3, where the RSM-PWIA results of fig. 2 are compared with the DWIA approaches previously outlined.

We see that FSI effects produce a reduction of the cross section, with respect to PWIA. The RMF and real ROP curves are quite similar, showing a reduction of about 30 ÷ 40% for  $E_\nu = 200$  MeV and 20% for the other energy values. In the case of the complex ROP model, instead, the reduction of the cross section is rather large, between 60% ( $E_\nu = 200$  MeV) and 50% (at higher energy), due to the absorption introduced by the imaginary term.

Let us note that the resonant structure appearing at high  $T_\mu$  is due to the use of real potentials (RMF and real ROP) for describing the final nucleon state. Here we only include single-particle excitations within a mean field picture, while including residual interactions would make the width and number of resonances to be considerably larger.

Finally, the results of figures 2 and 3 are summarized in fig. 4, where the cross section  $\sigma$ , integrated over the muon energy, is plotted as a function of the incident neutrino energy  $E_\nu$ . Again we see that within the PWIA the discrepancy between different

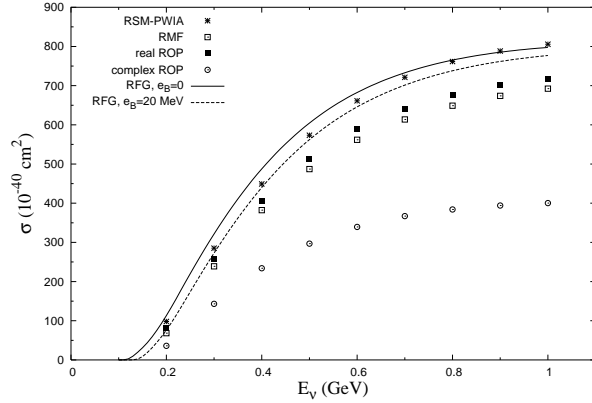


Figure 4. Integrated cross section  $\sigma$  for the quasi-elastic scattering of muon neutrinos on  $^{16}\text{O}$  as a function of the incident neutrino energy. The curves are calculated within the RFG model, while the points correspond to RSM calculations without FSI (stars) and with FSI effects taken into account within the RMF (empty squares), real ROP (full squares) and complex ROP (circles) approaches.

nuclear models is relatively small and decreases with increasing neutrino energy, while FSI effects are still present even at large  $E_\nu$ . The (more reliable) results for the RMF and real ROP approaches show a not too large, but still appreciable reduction ( $\sim 15\%$  at  $E_\nu = 1$  GeV), while, again, the imaginary term in the complex ROP leads to a too large reduction ( $\sim 50\%$ ) of the cross section.

In conclusion, within the Impulse Approximation, we observe that when FSI effects are neglected, the nuclear model dependence of the quasielastic  $\nu$ -nucleus cross section is large at low neutrino energy but becomes negligible at  $E_\nu = 1$  GeV. FSI effects are also rather large at  $E_\nu \simeq 200$  MeV and decrease with increasing neutrino energy, but, in the more realistic real ROP approach, can still be as large as 15 % at  $E_\nu = 1$  GeV and thus must be carefully considered.

As a final remark, we notice that if we consider Neutral Current quasielastic processes, where the outgoing nucleon must be detected, then using the complex ROP description of FSI would be more appropriate. Therefore in this case rather large FSI effects are expected to be present even at relatively high neutrino

energy [3,8].

## REFERENCES

1. G. P. Zeller, arXiv:hep-ex/0312061 and references therein.
2. see for example the contributions by O. Benhar and by C. Giusti to these proceedings.
3. W. M. Alberico *et al.*, Nucl. Phys. A 623, (1997) 471; Phys. Lett. B 438 (1998) 9.
4. J.M. Udías *et al.*, Phys. Rev. C 48 (1993) 2731; Phys. Rev. C 51 (1995) 3246; Phys. Rev. C 53 (1996) R1488; Phys. Rev. C 64 (2001) 024614.
5. C. Maieron, M.C. Martínez, J.A. Caballero, J.M. Udías, Phys. Rev. C 68 (2003) 048501.
6. C. Bleve *et al.*, Astropart. Phys. 16 (2001) 145; G. Cò, C. Bleve, I. De Mitri and D. Martello, Nucl. Phys. Proc. Suppl. 112 (2002) 210.
7. A. Meucci, C. Giusti and F. D. Pacati, Nucl. Phys. A 739 (2004) 277.
8. A. Meucci, C. Giusti and F. D. Pacati, arXiv:nucl-th/0405004.